Tilsner et al., http://www.jcb.org/cgi/content/full/jcb.201304003/DC1

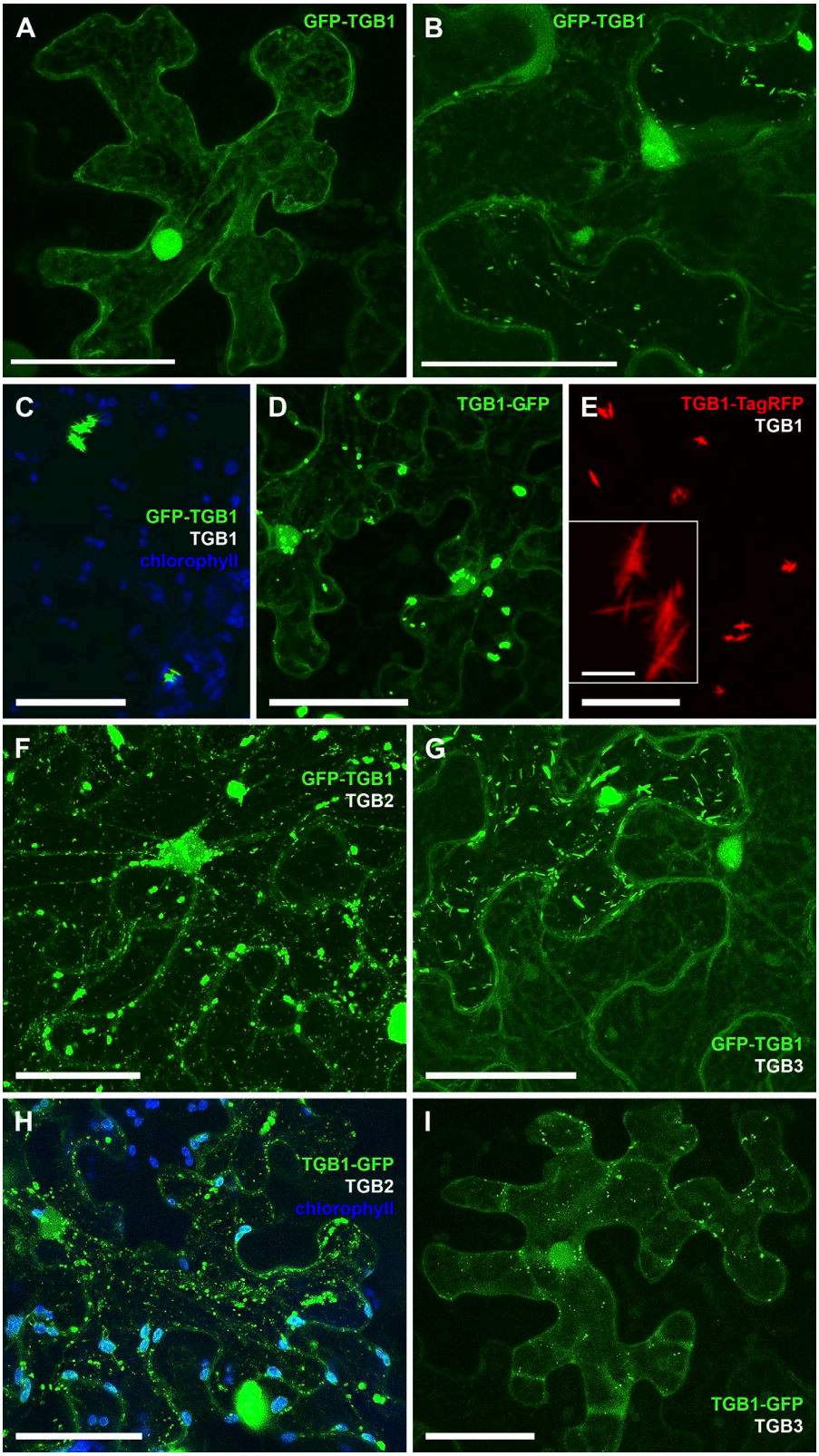

Figure S1. **TGB1 does not target PD by itself and is not recruited by TGB2 or TGB3 alone.** (A and B) GFP-TGB1 is cytoplasmic at 1 dpi (A) and starts to form aggregates at 2 dpi (B). (C) Presence of unfused TGB1 leads to aggregation of GFP-TGB1 but no PD are labeled. (D) TGB1-GFP labels aggregates and the cytoplasm. (E) TGB1-TagRFP forms aggregates in the presence of unfused TGB1 but does not localize to PD. Inset is a magnification of the needle-shaped TGB1-TagRFP aggregates also shown in the main image, to make their structure more apparent. (F and G) Neither TGB2 nor TGB3 alone can recruit GFP-TGB1 to PD. (H and I) Neither TGB2 nor TGB3 alone can recruit TGB1-GFP to PD. In C and H, chloroplast autofluorescence is shown in blue. All images are maximum projections of entire z stacks. Bars: (A–E [main image] and F–I) 50 µm; (E, inset) 10 µm.

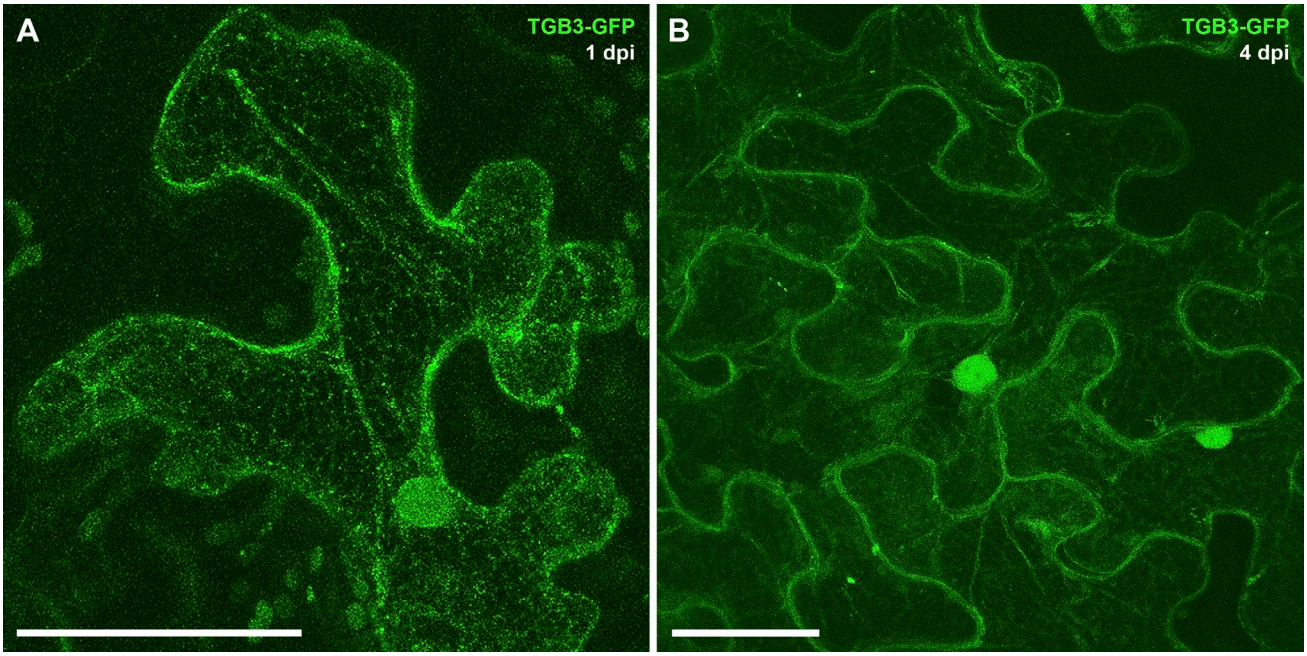

Figure S2. **TGB3-GFP does not target PD in the absence of unfused TGB3 protein.** (A and B) TGB3-GFP labels the ER at 1 dpi (A) and is mostly cytoplasmic at 4 dpi (B). (The fusion protein is unstable; Ju et al., 2008; Lee et al., 2010). Images are maximum projections of entire z stacks. Bars, 50 µm.

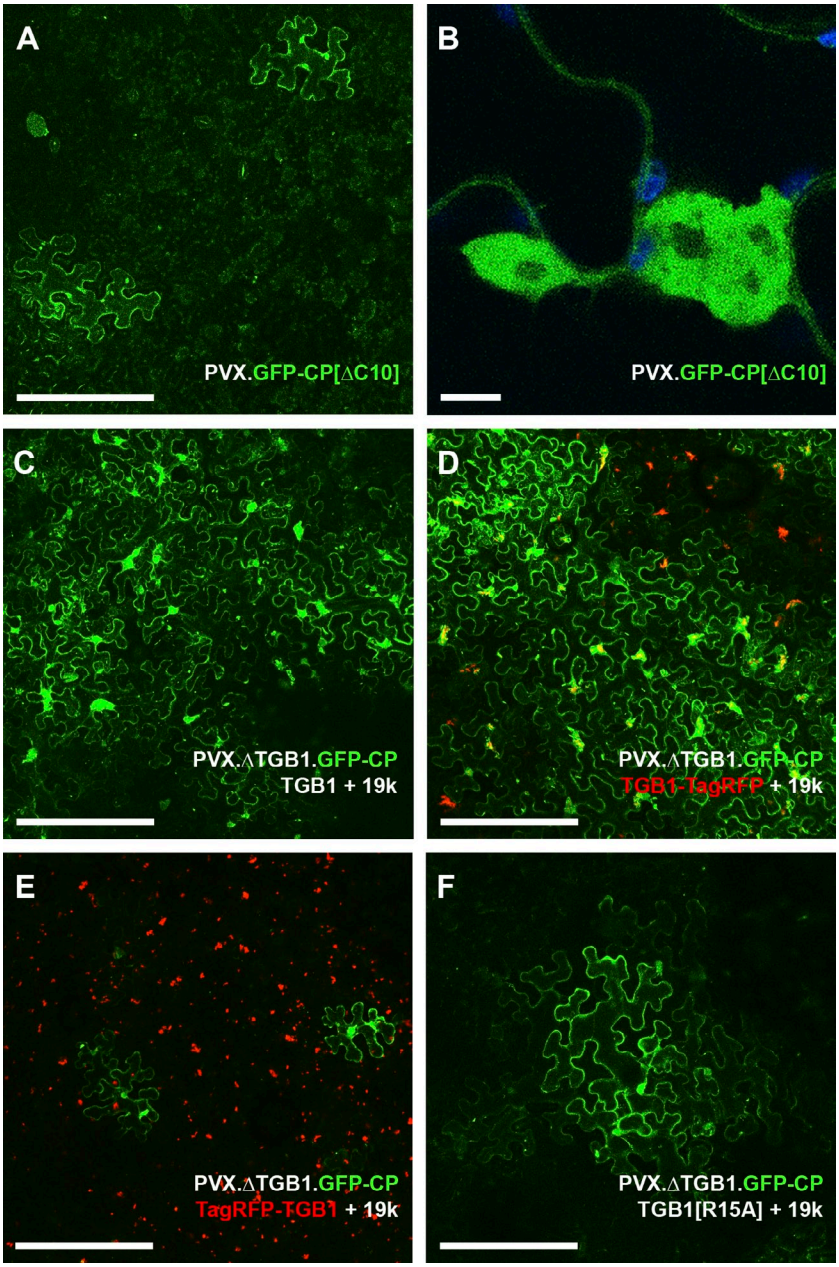

Figure S3. **PVX.GFP-CP[ΔC10] phenotype and TGB1 movement complementations (3 dpi).** White letters indicate coexpression of unfused proteins. 19k: ectopic silencing suppressor to compensate for potential effects of suppression deficiency in TGB1 mutants (Voinnet et al., 2003; Bayne et al., 2005). (A) PVX.GFP-CP[ΔC10] is movement deficient. (B) PVX.GFP-CP[ΔC10] forms perinuclear VRCs. (C) Unfused TGB1 rescues movement of TGB1-deficient PVX. (D) C-terminal TGB1-TagRFP also rescues movement of PVX.ΔTGB1.GFP-CP. (E) N-terminal TagRFP-TGB1 does not rescue PVX.ΔTGB1.GFP-CP movement. (F) TGB1[R15A] only partially restores PVX movement. In B, chloroplast autofluorescence is shown in blue. All images are maximum projections of entire z stacks except B, which is an individual z section. Bars: (A and C–F) 250 µm; (B) 10 µm.

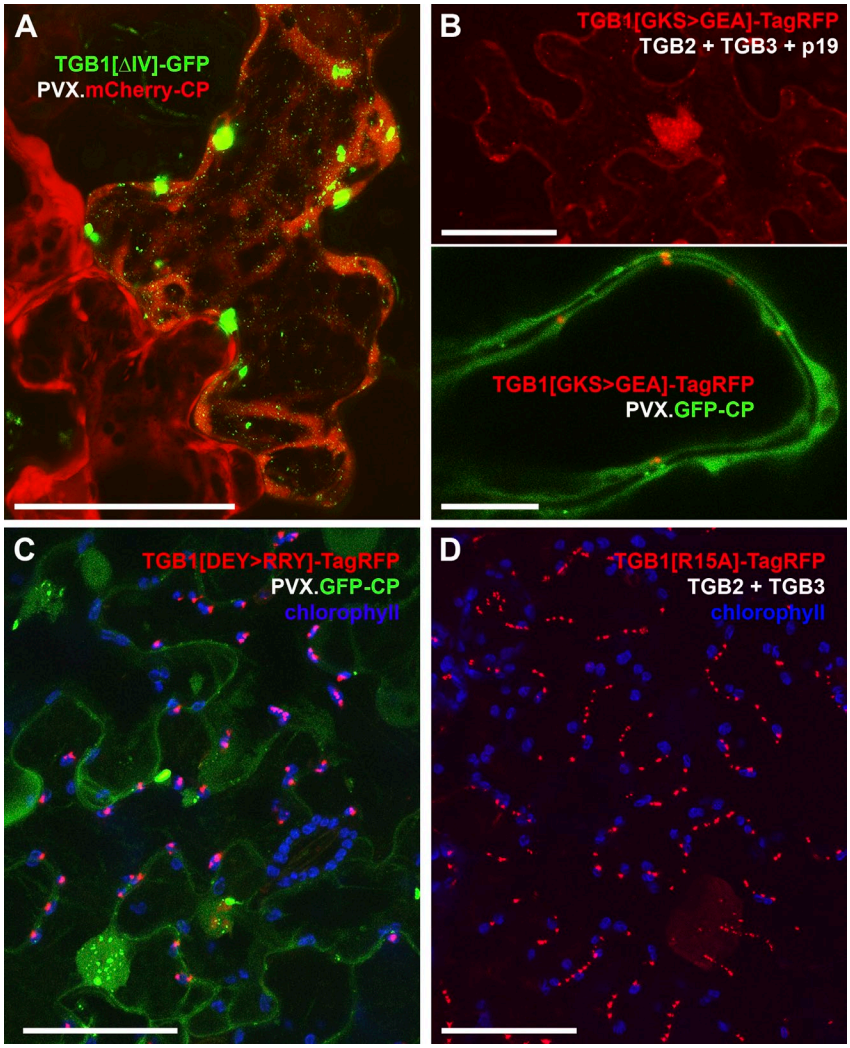

Figure S4. **PD recruitment of TGB1 mutants.** (A–C) TGB1[ΔIV]-GFP, TGB1[GKS to GEA]-TagRFP, and TGB1[DEY to RRY]-TagRFP are not PD localized in infected cells or by TGB2/3. p19: Tomato bushy stunt virus silencing suppressor to boost expression (Voinnet et al., 2003). (D) TGB1[R15A]-TagRFP is recruited to PD by TGB2 and 3. In C and D, chloroplast autofluorescence is shown in blue. All images are maximum projections of entire z stacks, except B [bottom image], which is an individual z section. Bars: (A, B [top], C, and D) 50 µm; (B, bottom) 10 µm.

Table S1. **Summary of PD targeting by combinations of TGB proteins**

TGB combination	TGB2/3 PD caps	TGB1 inside PD	Other comments/description
TGB1 PD targeting			
FP-TGB1	n.a.	No	Nuclear/cytoplasmic at low levels. At higher levels, forms elongated aggregates (Fig. S2, A and B)
FP-TGB1 + TGB1	n.a.	No	Needle-shaped aggregates (Fig. S2 C)
TGB1-FP	n.a.	No	Irregular aggregates (Fig. S2 D)
TGB1-FP + TGB1	n.a.	No	Needle-shaped aggregates (Fig. S2 E)
TGB2 PD targeting			
FP-TGB2	Yes	n.a.	Initially ER and PD; at higher expression levels, ER and granules (Fig. 3, A–C)
FP-TGB2 + TGB2	Yes	n.a.	No difference to FP-TGB2 alone (unpublished data)
TGB3 PD targeting			
TGB3-FP	No	n.a.	ER labeling at low expression levels and then fluorescence increasingly cytoplasmic (fusion unstable; Fig. S3, A and B; Ju et al., 2008; Lee et al., 2010)
TGB3-FP + TGB3	Yes	n.a.	ER-associated punctae and PD caps (Fig. 3 D)
Influence of TGB2 on TGB3 PD targeting			
TGB3-FP + TGB3 + TGB2	Yes	n.a.	Size and frequency of caps markedly increased compared to without TGB2 (Fig. 3 E)
PD recruitment of C-terminal TGB1 fusions by TGB2/3; effect of TGB2/TGB3 ratio			
TGB1-FP + TGB2	n.a.	No	No effect (Fig. S2 H)
TGB1-FP + TGB3	n.a.	No	No effect (Fig. S2 I)
TGB1-FP + TGB2 + TGB3 (1:1:1)	n.a.	Yes	Aggregates and PD (Fig. 3 F)
TGB1-FP + TGB2 + TGB3 (10:10:1)	n.a.	Yes	Aggregates and PD (unpublished data)
TGB1-FP + TGB2/3 bicistronic (10:10:1)	n.a.	Yes	Aggregates and PD (Fig. 3 G)
PD recruitment of N-terminal TGB1 fusions by TGB2/3			
FP-TGB1 + TGB2	n.a.	No	TGB1 aggregates more dispersed (Fig. S2 F)
FP-TGB1 + TGB3	n.a.	No	No effect (Fig. S2 G)
FP-TGB1 + TGB2 + TGB3	n.a.	Yes	Aggregates and PD (Fig. 3 H)
PD recruitment of C-terminal TGB1 fusions by fusions of TGB2 and 3			
TGB1-RFP + GFP-TGB2 + TGB3	Yes	No	Unpublished data
TGB1-RFP + GFP-TGB2 + TGB2 + TGB3	Yes	Yes	Fig. 4, A, C, and D
TGB1-RFP + TGB1 + GFP-TGB2 + TGB3	Yes	No	Unpublished data
TGB1-RFP + TGB2 + TGB3-GFP	No	No	Unpublished data
TGB1-RFP + TGB2 + TGB3-GFP + TGB3	Yes	Yes	Fig. 4, B and E
TGB1-RFP + TGB1 + TGB2 + TGB3-GFP	Yes	Yes	Weak TGB1-RFP labeling of PD (unpublished data)
PD recruitment of N-terminal TGB1 fusions by fusions of TGB2 and 3			
RFP-TGB1 + GFP-TGB2 + TGB3	Yes	No	Unpublished data
RFP-TGB1 + GFP-TGB2 + TGB2 + TGB3	Yes	Yes	Unpublished data
RFP-TGB1 + TGB2 + TGB3-GFP	No	No	Unpublished data
RFP-TGB1 + TGB2 + TGB3-GFP + TGB3	Yes	Yes	Unpublished data

n.a., not applicable.

Table S2. **Oligonucleotide primers used in this study**

Name	Sequence (5′ → 3′)
Generation of 35S::PVX.GFP-CP[ΔC10]	
PVX6809for	CCTGAGCACAAATTCGCTGC
dC10rev	AGACGTAGTTA–GGTTGTTGTTCCAGTGATACGACC
dC10for	ACTGGAACAACAACC–TAACTACGTCTACATAACCGACGCC
PVX7407rev	GCACCCCAGGCTTTACACTTTATG
TGB expression constructs	
attB-TGB2for	GGGGACAAGTTTGTACAAAAAAGCAGGCTGC–ATGTCCGCGCAGGGC
attB-TGB3for	GGGGACAAGTTTGTACAAAAAAGCAGGCTGC–ATGGAAGTAAATACATATCTCAACGC
attB-TGB3rev	GGGGACCACTTTGTACAAGAAAGCTGGGTA–ATGGAAACTTAACCGTTCAACG
attB-%TGB3rev	GGGGACCACTTTGTACAAGAAAGCTGGG–TTAATGGAAACTTAACCGTTCAACG
attB-TGB1for	GGGGACAAGTTTGTACAAAAAAGCAGGCTGC–ATGGATATTCTCATCAGTAGTTTGAAAAG
attB-TGB1rev	GGGGACCACTTTGTACAAGAGAAAGCTGGGTC–TGGCCCTGCGCGG
attB-%TGB1rev	GGGGACCACTTTGTACAAGAGAAAGCTGGGTC–CTATGGCCCTGCGCGG
TGB1[ΔIV] mutagenesis	
ΔIVfor	AGCCTAGAGCCCCAC–AGGAAAGTGGCAGATTTGATAGCTG
ΔIVrev	ATCTGCCACTTTCCT–GTGGGGCTCTAGGCTAAACTCC
TGB1[GKS to GEA] mutagenesis	
KSEAfor	CCGGTGAGGCCACAGCCCTAAGGAAGTTG
KSEArev	GGCTGTGGCCTCACCGGCTCCGG
TGB1[DEY to RRY] mutagenesis	
DERRfor	CGCAATCCTCCGTCGGTATACTTTGGACAAC
DERRrev	GTCCAAAGTATACCGACGGAGGATTGCGAAG
TGB1[R15A] mutagenesis	
R15Afor1	GTTTGAAAAGTTTAGGTTATTCTGCAACTTCCAAATC
R15Afor2	ATGGATATTCTCATCAGTAGTTTGAAAAGTTTAGGTTATTCTGCAAC
GFP-CP and CP expression	
attB-CPfor	GGGGACAAGTTTGTACAAAAAAGCAGGCTGC–ATGTCAGCACCCGCGAGCACAACAC
attB-CPrev	GGGGACCACTTTGTACAAGAGAAAGCTGGG–TTATGGTGGTGGTAGAGTGACAA
165k$^{[1\text{-}997]}$-GFP expression	
attB-165kfor	GGGGACAAGTTTGTACAAAAAAGCAGGCTGC–ATGGCCAAGGTGCGCG
attB-165kHELrev	GGGGACCACTTTGTACAAGAGAAAGCTGGGTC–GTACTCCCTGAGTGCTTGTTCTCTC

Percentage signs denote primers with stop codons. Gateway adapters and gene-specific sequences, as well as gene-specific sequences flanking deletions, are separated by dashes. Relevant mutagenic nucleotides and stop codons are underlined. for, forward; rev, reverse.

References

Bayne, E.H., D.V. Rakitina, S.Y. Morozov, and D.C. Baulcombe. 2005. Cell-to-cell movement of potato potexvirus X is dependent on suppression of RNA silencing. *Plant J.* 44:471–482. http://dx.doi.org/10.1111/j.1365-313X.2005.02539.x

Ju, H.-J., C.M. Ye, and J. Verchot-Lubicz. 2008. Mutational analysis of PVX TGBp3 links subcellular accumulation and protein turnover. *Virology*. 375:103–117. http://dx.doi.org/10.1016/j.virol.2008.01.030

Lee, S.-C., C.-H. Wu, and C.-W. Wang. 2010. Traffic of a viral movement protein complex to the highly curved tubules of the cortical endoplasmic reticulum. *Traffic*. 11:912–930. http://dx.doi.org/10.1111/j.1600-0854.2010.01064.x

Voinnet, O., S. Rivas, P. Mestre, and D. Baulcombe. 2003. An enhanced transient expression system in plants based on suppression of gene silencing by the p19 protein of tomato bushy stunt virus. *Plant J.* 33:949–956. http://dx.doi.org/10.1046/j.1365-313X.2003.01676.x